Accepted Manuscript

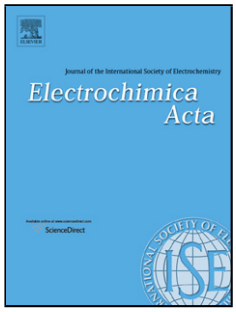

Title: Azafluorene Ornamented Thiazine Based Novel Fused Heterocyclic Organic Dyes for Competent Molecular Photovoltaics

Authors: Kesavan Stalindurai, Ayyanar Karuppasamy, Jia-De Peng, Kuo-Chuan Ho, Chennan Ramalingan

PII: S0013-4686(17)31389-0
DOI: http://dx.doi.org/doi:10.1016/j.electacta.2017.06.151
Reference: EA 29789

To appear in: *Electrochimica Acta*

Received date: 30-1-2017
Revised date: 15-5-2017
Accepted date: 24-6-2017

Please cite this article as: Kesavan Stalindurai, Ayyanar Karuppasamy, Jia-De Peng, Kuo-Chuan Ho, Chennan Ramalingan, Azafluorene Ornamented Thiazine Based Novel Fused Heterocyclic Organic Dyes for Competent Molecular Photovoltaics, Electrochimica Actahttp://dx.doi.org/10.1016/j.electacta.2017.06.151

This is a PDF file of an unedited manuscript that has been accepted for publication. As a service to our customers we are providing this early version of the manuscript. The manuscript will undergo copyediting, typesetting, and review of the resulting proof before it is published in its final form. Please note that during the production process errors may be discovered which could affect the content, and all legal disclaimers that apply to the journal pertain.

ACCEPTED MANUSCRIPT

Azafluorene Ornamented Thiazine Based Novel Fused Heterocyclic Organic Dyes for Competent Molecular Photovoltaics

Kesavan Stalindurai[a], Ayyanar Karuppasamy[a], Jia-De Peng[b], Kuo-Chuan Ho[b,*], Chennan Ramalingan[a,*]

[a] *Department of Chemistry, Kalasalingam University, Krishnankoil – 626 126, Tamilnadu, India*

[b] *Department of Chemical Engineering, National Taiwan University, Taipei 10617, Taiwan*

Corresponding author E-mail: ramalinganc@gmail.com (C. Ramalingan), kcho@ntu.edu.tw (K.-C. Ho)

GRAPHICAL ABSTRACT

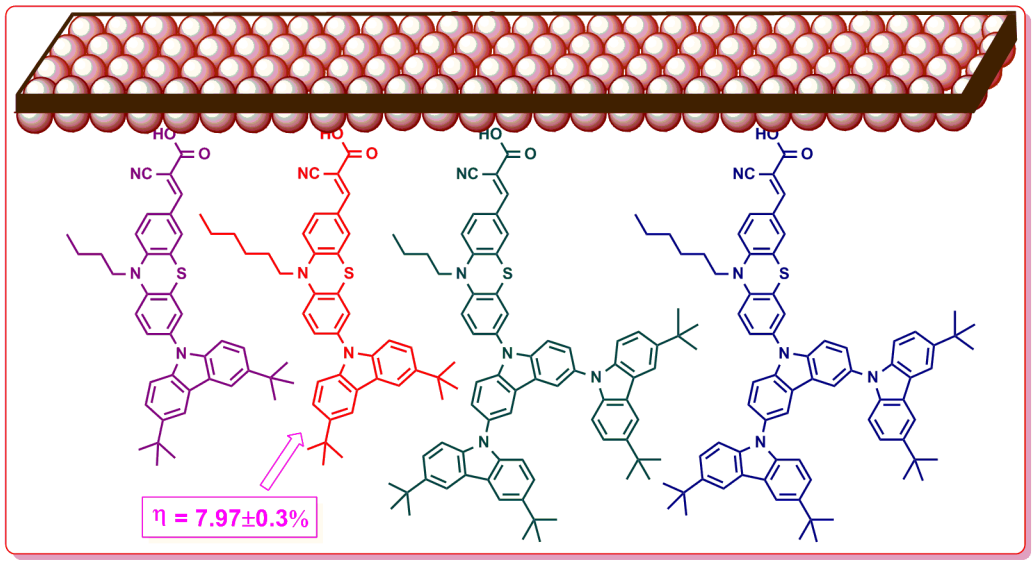

HIGHLIGHTS

- A series of azafluorene and thiazine based fused heterocyclic dyes has been synthesized.
- Photophysical / electrochemical behaviors of the dyes have been examined.
- Computational study - well separated distribution of electrons in donor and acceptor motifs.
- The dye TBCPCA-2 carrying device exhibited the highest power conversion efficiency.

ACCEPTED MANUSCRIPT

ABSTRACT

Described herein is a series of azafluorene ornamented thiazine based novel fused heterocyclic organic dyes **TBCPCA-1**, **TBCPCA-2**, **TBTCPCA-1** and **TBTCPCA-2**. Nanocrystalline titania based DSSC performance along with photophysical / electrochemical behaviors of the aforementioned dyes have been examined. Utilizing computational approach, distribution of electrons within the molecules has been explored. The devices possessing the novel fused dyes **TBCPCA-1**, **TBCPCA-2**, **TBTCPCA-1** and **TBTCPCA-2** as sensitizers exhibited overall power conversion efficiency range between 6.17±0.4 and 7.97±0.3%. The novel fused heterocyclic organic dyes featuring di-*tert*-butylazafluorene structural motif such as **TBCPCA-1** and **TBCPCA-2** exhibit higher power conversion efficiency than the ones carrying sterically congested tetra-*tert*-butyl-tri(azafluorene) scaffold viz., **TBTCPCA-1** and **TBTCPCA-2**. Amongst the devices fabricated with the utilization of novel heterocyclic dyes as sensitizers, the device possessing the dye **TBCPCA-2** as sensitizer displayed the highest power conversion efficiency of 7.97±0.3% along with a V_{oc} of 745±0.6 mV, a J_{sc} of 16.92±0.3 mA.cm^{-2} and a *ff* of 0.67±0.003.

Keywords: Azafluorene, Heterocycles, Organic dyes, Solar cells, Powerconversion efficiency

1. Introduction

In recent years, growing energy hassle and issue regarding global-warming make great focal point of the scientists on the sources of renewable energy. To address these concerns, inexorable research efforts have been committed to DSSCs [1-6], feature of an inter-connected system of large band-gap nano semi-conducting materials, from materials syntheses, device-physics and interface-engineering features. The efficiency of the DSSCs is fundamentally

ACCEPTED MANUSCRIPT

affected by the sensitizer, the anode, the cathode, and the electrolyte. Of the factors that affect significantly the device power conversion efficiency, the dyes participate a vital part for DSSCs to achieve high PCE [7,8]. Conventionally, DSSCs with elevated PCEs were first accomplished with Ru-polypyridyl based sensitizers [9-19], whose performances were soon after exceeded by Zn-porphyrin based dyes [3,7]. Although the aforementioned ones are efficient sensitizers, they have their own limitations. Specifically, a Ru-based dye has draw-backs of source paucity and toxicity while Zn-porphyrin dye obtained in lower yield and requires awfully lethal reactants/reagents. Thus, sensitizers with no metals, which possess D-π-A architecture, have also fascinated attention due to molecular design flexibility, raw materials abundance, economic suppleness, and bright colours [20-24]. It has recently been described that electrons (injected) recombination with the dye (oxidized) / electrolyte rigorously reduces photo-current density [25]. Vitally, the ability of organic DSSCs is reliant on its structural and electronic distinctiveness [26-33]. On comparing the semiconductor (CB) energy, the LUMO energy of the dyes has to be superior for the thermodynamic possibility of charge injection whereas for the charge generation, the dyes having strong and broader charge-transfer absorption are favorable [31]. Hence, several structural modifications including incorporation of alkyl chains have been made to encumber the reactions with recombination and participate to the raise in J_{sc} and V_{oc} of the devices of DSSCs [34-37]. In this context, DSSCs with various types of metal-free dyes as sensitizers have been constructed and offered appreciable efficiencies [38-41]. This demonstrates the great potential of organic dyes as efficient DSSC sensitizers. Although various types of organic dyes have been documented as DSSC sensitizers, synthesis of novel organic dyes as efficient sensitizers is still desired.

ACCEPTED MANUSCRIPT

Figure 1

Metal free materials possessing azafluorene / thiazine based fused heterocycles have been utilized as building blocks in a diverse range of electronic devices which include OLEDs and DSSCs [42-60]. The first thiazine based fused heterocycle and cyanoacrylic acid structural motifs possessing organic dye has been reported with PCE of 5.5% by Hagfeldt and Sun *et al* in 2007 [61] wherein N-butyl thiazine based fused heterocyclic structural motif play a role of donor and acrylic acid scaffold serve as acceptor **(A)** (Figure 1). Besides, it is recognized that substituted amine functionalities serve as competent electron donors in DSSCs and a diverse range of organic dyes possessing amine functionalities as donors has been documented in the literature. Since 2007, various types of amine functionalities on 6-position of thiazine based fused heterocyclic unit **(**i.e., in **A)** have been introduced by several research groups around the globe **(A1-A7)** and achieved power conversion efficiencies up to 7.1% [62-64]. We herein construct four azafluorene ornamented thiazine based novel fused heterocyclic organic dyes wherein di-*tert*-butylazafluorene / sterically conjested tetra-*tert*-butyltri(azafluorene) as donors, alkylsubstituted fused thiazines as spacers, and acrylic acid as an acceptor as illustrated in Figure 2. We initially hypothesized that introduction of azafluorene / multi-azafluorenes would improve the electron donating ability besides extending π-conjugation and, further incorporation of di / multi *tert*-butyl bulky groups on azafluorene scaffold would restrain the intermolecular aggregation, enhance the solubility and increases the light resistant capability of the dyes [50,65-68]. The electron rich nitrogen and sulfur in fused thiazine structural motif would also facilitate the donation of electrons in a competent manner. The non-planar butterfly conformation of the thiazine ring of fused heterocyclic moiety would hamper aggregation of the dye and the

ACCEPTED MANUSCRIPT

formation of intermolecular excimers besides the long chain alkyl group which would enhance the solubility and control the aggregation [36,58,61]. Further, the π-delocalization of fused aryl groups would extend over the complete thiazine possessing aromatic chromophore as two fused aryl moieties in the same are set in an undersized angle (torsion) associated with sulfur and nitrogen atoms. Eventually, incorporation of cyanoacrylic acid would competently accept/withdraw the electrons and also graft on the TiO_2 oxide layer.

Figure 2

2. Experimental Section

2.1. General

Standard procedures were utilized for distilling /drying the solvents. Reagent quality reagents were purchased and used as such. Pre-silica coated aluminium plates (60, F_{254}) were utilized for TLC and the solvents specified were used as eluents. Column-Chromatography was carried-out on Silica gel (spherical, 100-200 mesh) slurry packed in glass columns. The eluting solvents employed for respective separations are provided in the individual experimental procedures section. NMR spectra were acquired on a Bruker 400 MHz NMR spectrometer at 25 °C. Internal standard used for the NMR measurements was tetramethylsilane (TMS) while deuterated chloroform was used as a solvent. Shimadzu IR Tracer-100 instrument in the range of 4000-400 cm^{-1} was utilized to record FT-IR spectra and samples with KBr pellet form were utilized for recording the same. The IR spectral features are reported in wave number (cm^{-1}). VarioMICRO system was utilized for microanalyses. Cyclic voltametry experiments were executed at ambient temperature using a three-electrode (conventional) configuration. The three

ACCEPTED MANUSCRIPT

electrodes used are glassy carbon as a working electrode, $Ag/AgNO_3$ as a reference electrode, and a platinum wire as an auxiliary electrode. The $E_{(1/2)}$ figures were determined using $1/2(E^a_p + E^c_p)$ in which E^a_p is the anodic peak potential and E^c_p is the cathodic peak potential. Ferrocene was used as a standard (internal) and the potentials were indicated with respect to the same. The solvent and supporting electrolyte in all the experiments were dichloromethane and 0.1M tetrabutylammonium perchlorate, respectively. JASCO V-650 UV-Vis spectrophotometer with freshly prepared solutions was used for recording the absorption spectra. Guassian 09 program [DFT, B3LYP; 6-311++G(d,p)] package was utilized for computational calculations.

2.2. Synthetic methodologies

The intermediates, diiodoazafluorene **2**, N-tosyl diiodoazafluorene **3**, di-*tert*-butylazafluorene **4**, N-tosyl-tetra-*tert*-butyl-tri(azafluorene) **5**, tetra-*tert*-butyl-tri(azafluorene) **6**, N-alkyl fused thiazines (**8** and **9**), carbaldehydes of N-alkyl fused thiazines (**10** and **11**), and bromocarbaldehydes of fused thiazines (**12** and **13**) were synthesized by adopting the literature methods [69-71].

*2.2.1. Synthesis of carbaldehyde **14***

Bromocarbaldehyde of fused thiazine **12** (0.50 g, 1.38 mmol), di-tert-butylazafluorene **4** (0.39 g, 1.38 mmol), K_2CO_3 (0.6 g, 4.34 mmol), copper-bronze (0.14 g, 2.16 mmol), and 18-crown-6 (0.06 g, 0.20 mmol) were charged in a double neck RB flask (100 mL) equipped with reflux condenser under nitrogen atmosphere. Solvent *ortho*-dichlorobenzene (ODCB) (20 mL) was then added using a syringe and stirred for

ACCEPTED MANUSCRIPT

two minutes. The temperature was raised to reflux while stirring and it was continued for 48h. It was then filtered after cooling so as to eliminate the insoluble inorganic material. The solid inorganic material was washed further with DCM (3x30 mL). The washed solvent and the already collected filtrate were united and the same was washed with dilute aq. NH_3 followed by water. The organic-phase was dried using Mg_2SO_4, filtered and the solvent was evaporated to furnish the crude sample. Column chromatographic separation of the crude sample using hexane-dichloromethane mixture (4:6) eventually furnished the pure title compound. Yield: 0.56 g (73%), m.p. 218-220°C. ^{1}H NMR (400 MHz, $CDCl_3$, 25°C, TMS): δ = 1.01 (t, *J* = 7.40Hz, 3H), 1.45 (s, 18H), 1.63-1.52 (m, 2H), 1.92-1.85 (m, 2H), 3.97 (t, *J* = 7.20Hz, 2H), 6.97 (d, *J* = 8.40Hz, 1H), 7.04 (d, *J* = 6.00 Hz, 1H), 7.34-7.26 (m, 4H), 7.47-7.44 (m, 2H), 7.62 (s, 1H), 7.70-7.68 (m, 1H), 8.12 (d, *J* = 1.20Hz, 2H), 9.82 (s, 1H). ^{13}C NMR (100 MHz, $CDCl_3$. 25°C, TMS): δ = 13.84, 20.18, 29.74, 32.04, 34.77, 47.99, 109.12, 115.03, 116.29, 116.59, 123.30, 123.65, 124.50, 125.36, 125.69, 125.88, 128.65, 130.24, 131.31, 133.81, 139.25, 142.34, 142.94, 150.39, 190.00; IR (KBr, cm^{-1}): ν 424.3, 470.6, 505.4, 543.9, 572.9, 611.4, 651.9, 738.7, 801.1, 879.5, 920.1, 1029.9, 1101.4, 1143.8, 1197.8, 1236.4, 1257.6, 1294.2, 1325.1, 1363.7, 1410.0, 1471.7, 1579.7, 1602.9, 1693.5, 2860.4, 2955.0, 3055.2; elemental analysis calcd (%) for $C_{37}H_{40}N_2OS$: C 79.24, H 7.19, N 5.00, S 5.72; found: C 79.43, H 7.22, N 4.96, S 5.69.

*2.2.2. Synthesis of carbaldehyde **15***

A mixture of bromocarbaldehyde of fused thiazine **13** (0.54 g, 1.38 mmol), di-*tert*-butylazafluorene **4** (0.39 g, 1.38 mmol), K_2CO_3 (0.60 g, 4.34 mmol), copper-bronze (0.14 g, 2.16 mmol), and 18-crown-6 (0.06 g, 0.20 mmol) in ODCB (20 mL) gave the title compound by

ACCEPTED MANUSCRIPT

adopting the above method. Yield: 0.54 g (67%), m.p. 227-229°C. ^{1}H NMR (400 MHz, $CDCl_3$, 25°C, TMS): δ = 0.90 (t, *J* = 4.40Hz, 3H), 1.49-1.32 (m, 4H), 1.46 (s, 18H), 1.61-1.59 (m, 2H), 1.91-1.87 (m, 2H), 3.94 (t, *J* = 7.20Hz, 2H), 6.94 (d, *J* = 8.40Hz, 1H), 7.02 (d, *J* = 8.40Hz, 1H), 7.31-7.25 (m, 4H), 7.46-7.44 (m, 2H), 7.61 (s, 1H), 7.68 (d, *J* = 2.00Hz, 1H), 8.13 (d, *J* = 1.60Hz, 2H), 9.81 (s, 1H). ^{13}C NMR (100 MHz, $CDCl_3$, 25°C, TMS): δ = 14.05, 22.63, 26.60, 26.79, 31.45, 32.06, 34.77, 48.30, 109.13, 115.02, 116.30, 116.60, 123.31, 123.66, 124.46, 125.35, 125.67, 125.88, 128.63, 130.26, 131.29, 133.79, 139.25, 142.31, 142.94, 150.38, 190.02; IR (KBr, cm^{-1}): ν 424.3, 468.7, 543.9, 611.4, 651.9, 736.8, 810.1, 881.5, 920.1, 1029.9, 1101.4, 1143.8, 1197.8, 1255.7, 1294.2, 1327.0, 1363.7, 1409.9, 1471.7, 1579.7, 1602.9, 1693.5, 2860.4, 2956.9, 3055.2; elemental analysis calcd (%) for $C_{39}H_{44}N_2OS$: C, 79.55; H, 7.53; N, 4.76; S, 5.45. Found: C, 79.81; H, 7.61; N, 4.73; S, 5.43.

*2.2.3. Synthesis of carbaldehyde **16***

A mixture of bromocarbaldehyde of fused thiazine **12** (0.25 g, 0.69 mmol), tetra-*tert*-butyl-tri(azafluorene) **6** (0.50 g, 0.69 mmol), K_2CO_3 (0.30 g, 2.17 mmol), copper-bronze (0.07 g, 1.08 mmol), and 18-crown-6 (0.03 g, 0.10 mmol) in ODCB (25 mL) provided the title compound by using the above method. Yield: 0.44 g (64%), m.p. 318-319°C. ^{1}H NMR (400 MHz, $CDCl_3$, 25°C, TMS): δ = 0.93 (t, *J* = 7.40Hz, 3H), 1.20-1.16 (m, 2H), 1.37 (s, 36H), 1.47-1.44 (m, 2H), 3.86 (t, *J* = 7.18Hz, 2H), 6.84 (d, *J* = 8.15Hz, 1H), 6.96 (d, *J* = 8.04Hz, 1H), 7.18 (s, 1H), 7.23 (d, *J* = 8.80Hz, 4H), 7.35-7.32 (m, 6H), 7.51-7.47 (m, 4H), 7.60 (s, 1H), 7.85 (d, *J* = 7.90Hz, 1H), 8.13-8.06 (m, 6H), 9.81 (s, 1H); ^{13}C NMR (100 MHz, $CDCl_3$, 25°C, TMS): δ = 13.83, 20.10, 29.79, 32.02, 34.74,

ACCEPTED MANUSCRIPT

47.97, 109.10, 115.01, 116.21, 116.51, 123.32, 123.62, 123.65, 123.77, 124.52, 124.85, 125.32, 125.62, 125.77, 125.82, 128.62, 130.23, 131.33, 133.83, 139.23, 142.34, 142.94, 150.35, 190.04; IR (KBr, cm^{-1}): ν 422.4, 468.7, 572.9, 611.4, 651.9, 738.7, 808.2, 877.6, 918.1, 1029.9, 1103.3, 1197.8, 1234.4, 1259.5, 1290.4, 1325.1, 1363.7, 1487.1, 1577.8, 1602.9, 1691.6, 2864.3, 2955.0, 3047.5; elemental analysis calcd (%) for $C_{69}H_{70}N_4OS$: C 82.59, H 7.03, N 5.58, S 3.20; found: C 82.85, H 6.99, N 5.60, S 3.22.

*2.2.4. Synthesis of carbaldehyde **17***

A mixture of bromocarbaldehyde of fused thiazine **13** (0.27 g, 0.69 mmol), tetra-*tert*-butyl-tri(azafluorene) **6** (0.5 g, 0.69 mmol), K_2CO_3 (0.30 g, 2.17 mmol), copper-bronze (0.07 g, 1.08 mmol), and 18-crown-6 (0.03 g, 0.10 mmol) in ODCB (25 mL) yielded the title compound by employing the above method. Yield: 0.48 g (68%), m.p. 332-334°C. ^{1}H NMR (400 MHz, $CDCl_3$, 25°C, TMS): δ = 0.89 (t, *J* = 4.00Hz, 3H), 1.24-1.22 (m, 2H), 1.30-1.27 (m, 4H), 1.40 (br.s, 40H), 3.92 (t, *J* = 7.35Hz, 2H), 6.82 (d, *J* = 8.12Hz, 1H), 6.93 (d, *J* = 7.95Hz, 1H), 7.20-7.17 (m, 4H), 7.47-7.40 (m, 6H), 7.68 (s, 1H), 7.96-7.93 (m, 1H), 8.25-8.13 (m, 6H), 9.82 (s, 1H); ^{13}C NMR (100 MHz, $CDCl_3$, 25°C, TMS): δ = 14.04, 22.62, 26.66, 26.76, 31.41, 32.02, 34.74, 48.38, 109.10, 115.01, 116.31, 116.61, 123.32, 123.62, 123.65, 123.80, 124.42, 124.91, 125.32, 125.62, 125.82, 125.83, 128.62, 129.95, 130.23, 131.05, 131.23, 133.73, 139.23, 142.38, 142.84, 150.35, 190.09; IR (KBr, cm^{-1}): ν 424.3, 468.7, 501.5, 547.8, 577.9, 611.4, 651.9, 738.7, 810.1, 879.5, 920.1, 1029.9, 1103.3, 1197.8, 1238.3, 1261.5, 1292.3, 1327.0, 1363.7, 1413.8, 1487.1, 1577.7, 1602.9, 1693.5, 2864.3, 2956.9, 3047.5; elemental analysis calcd (%) for $C_{71}H_{74}N_4OS$: C 82.68, H 7.23, N 5.43, S 3.11; found: C 82.86, H 7.26, N 5.40, S 3.13.

ACCEPTED MANUSCRIPT

*2.2.5. Synthesis of dye **TBCPCA-1***

A mixture of carbaldehyde **14** (0.22 g, 0.4 mmol) and cyanoacetic acid (0.04 g, 0.5 mmol) in the presence of ammoniam acetate (0.02 g, 0.22 mmol) in AcOH (15 mL) was refluxed for 12h. The mixture was diluted with water after cooling and extracted with DCM. The organic portion was separated, washed well with water, dried over Mg_2SO_4 and the solvent was removed. The crude thus obtained was subjected to column chromatographic separation utilizing 10% methanol in ethyl acetate as eluting system to eventually provide the title dye molecule. Yield: 0.20g, (79%), m.p. 165-166°C. ^{1}H NMR (400 MHz, $CDCl_3$, 25°C, TMS): δ = 1.04 (t, *J*=7.20Hz, 3H), 1.33-1.25 (m, 2H), 1.46 (s, 18H), 1.55-1.51 (m, 2H), 3.96 (t, *J*=7.00Hz, 2H), 6.92 (d, *J*=8.80Hz, 1H), 7.03 (d, *J*=8.75Hz, 1H), 7.31-7.26 (m, 5H), 7.46 (dd, *J*=8.40Hz, 1.60Hz, 2H), 7.96 (d, *J*=8.60Hz, 1H), 7.69(s, 1H), 8.12 (d, *J*=1.20Hz, 2H); ^{13}C NMR (400 MHz, $CDCl_3$, 25°C, TMS): δ = 13.83, 20.17, 29.74, 32.04, 34.77, 48.06, 98.18, 109.12, 115.19, 116.30, 116.58, 123.33, 123.69, 124.15, 124.85, 125.62, 125.69, 125.88, 130.66, 131.90, 134.06, 139.17, 141.68, 142.99, 149.79, 154.39, 167.90; IR (KBr, cm^{-1}): ν 2221.8 (C≡N); elemental analysis calcd (%) for $C_{40}H_{41}N_3O_2S$: C 76.52, H 6.58, N 6.69, S, 5.11; found: C 76.71, H 6.51, N 6.74, S 5.08.

*2.2.6. Synthesis of dye **TBCPCA-2***

The title dye molecule was synthesized using carbaldehyde **15** (0.24 g, 0.4 mmol) by employing the above method with no change in other reactants/reagents. Yield: 0.21g,

ACCEPTED MANUSCRIPT

(81%), mp. 200-202°C. ^{1}H NMR (400 MHz, $CDCl_3$, 25°C, TMS): δ = 0.89 (t, *J*=5.20Hz, 3H), 1.29-1.23 (m, 2H), 1.36-1.33 (m, 4H), 1.45 (br.s, 24H), 3.92 (t, *J*=6.80Hz, 2H), 6.90 (d, *J*=8.80Hz, 1H), 7.00 (d, *J*=8.40Hz, 1H), 7.19-7.17 (m, 3H), 7.46-7.42 (m, 3H), 7.67 (s, 1H), 7.94 (d, *J*=8.40Hz, 1H), 8.09 (s, 1H), 8.12 (s, 2H); ^{13}C NMR (100 MHz, $CDCl_3$, 25°C, TMS): δ = 14.04, 22.74, 26.58, 31.43, 32.05, 34.77, 48.38, 98.16, 109.14, 115.17, 115.96, 116.31, 116.59, 123.36, 123.70, 123.99, 124.12, 124.85, 125.58, 125.65, 125.86, 127.75, 130.57, 130.66, 131.98, 134.07, 139.18, 141.61, 143.01, 149.81, 154.47, 167.97; IR (KBr, cm^{-1}): ν 2217.4 (C≡N); elemental analysis calcd (%) for C42H45N3O2S: C 76.91, H 6.92, N 6.41, S 4.89; found: C 76.69, H 6.98, N 6.47, S 4.84.

2.2.7. Synthesis of dye ***TBTCPCA-1***

By utlilzing the above method, the title dye molecule was synthesized from the reaction of carbaldehyde **16** (0.40 g, 0.4 mmol) with no alteration in other reactants/reagents. Yield: 0.31g (73%), m.p. 260-261°C. ^{1}H NMR (400 MHz, $CDCl_3$, 25°C, TMS): δ = 0.93 (t, *J*=7.40Hz, 3H), 1.20-1.16 (m, 2H), 1.46 (s, 36H), 1.53-1.49 (m, 2H), 3.85 (t, *J*=6.80Hz, 2H), 6.83 (d, *J*=8.35Hz, 1H), 6.97 (d, *J*=8.35Hz, 1H), 7.17 (s, 1H), 7.25-7.22 (m, 4H), 7.37-7.33 (m, 6H), 7.51-7.49 (m, 4H), 7.61 (s, 1H), 7.88 (d, *J*=8.80Hz, 1H), 8.06 (s, 4H), 8.12 (s, 2H); ^{13}C NMR (100 MHz, $CDCl_3$, 25°C, TMS): δ = 13.86, 20.18, 29.74, 32.06, 34.75, 48.06, 98.16, 109.09, 111.07, 115.36, 116.25, 119.32, 123.12, 123.60, 123.92, 125.51, 126.00, 130.95, 131.87, 132.83, 140.10, 140.38, 142.59, 142.89, 149.79, 154.39, 167.94; IR (KBr, cm^{-1}): ν 2224.7 (C≡N); elemental analysis calcd (%) for $C_{72}H_{71}N_5O_2S$: C 80.79, H 6.69, N 6.54, S 3.00; found: C 81.06, H 6.62, N 6.59, S 3.03.

ACCEPTED MANUSCRIPT

*2.2.8. Synthesis of dye **TBTCPCA-2***

Synthesis of the title molecule was achieved from the reaction of carbaldehyde **17** (0.41 g, 0.4 mmol) by using the above method with no modification in other reactants/reagents. Yield: 0.30g (69%), m.p. 265-266°C. ^{1}H NMR (400 MHz, $CDCl_3$, 25°C, TMS): δ = 0.90 (t, *J*=5.10Hz, 3H), 1.29-1.23 (m, 2H), 1.36-1.32 (m, 4H), 1.45 (br.s, 38H), 3.92 (t, *J*=6.00Hz, 2H), 6.86 (d, *J*=8.40Hz, 1H), 6.96 (d, *J*=8.40Hz, 1H), 7.19-7.17 (m, 5H), 7.30-7.24 (m, 6H), 7.48-7.44 (m, 4H), 7.68 (s, 1H), 7.95 (d, *J*=8.00Hz, 1H), 8.09 (s, 4H), 8.17 (s, 2H); ^{13}C NMR (100 MHz, $CDCl_3$, 25°C, TMS): δ = 14.04, 22.62, 29.79, 31.41, 32.02, 34.74, 48.36, 98.17, 109.19, 115.15, 115.95, 116.36, 116.56, 123.33, 123.73, 123.93, 124.14, 124.84, 125.55, 125.65, 125.85, 127.77, 130.50, 130.60, 131.91, 134.04, 139.19, 141.61, 143.03, 149.89, 154.44, 167.92; IR (KBr, cm^{-1}): ν 2220.5 (C≡N); elemental analysis calcd (%) for $C_{74}H_{75}N_5O_2S$: C 80.91, H 6.88, N 6.38, S 2.92; found: C 80.67, H 6.94, N 6.33, S 2.88.

2.3. Fabrication of DSSC and characterization

A tin(IV) oxide conducting glass (fluorine doped; ~80% transmittance; 7 Ω sq^{-1}) was firstly cleaned utilizing a cleaner (neutral) and was then washed with water (deionized), afterward with dimethyl ketone and then with 2,3-dimethylbutan-2-ol. To reach good mechanical contact between the film of titanium(IV) oxide and the conducting glass, and also to isolate the surface of the glass (conducting) from the electrolyte, the conducting exterior of the FTO was treated with tetraisopropyl orthotitanate (1000 mg) in ethyleneglycol monomethyl ether (3000

ACCEPTED MANUSCRIPT

mg) solution. By employing doctor blade technique, titanium(IV) oxide paste was coated on the aforesaid glass. The dried titanium(IV) oxide film was steadily heated (450 °C) in O_2 atm. and accordingly sintered at the same temp. for 0.5 hour to coat each titanium(IV) oxide layer.

The titanium(IV) oxide photo-anodes of the DSSCs used in the tests were composed of a 15 μm thick transparent titanium(IV) oxide (13 nm) layer with a scattering titanium(IV) oxide (300 nm) layer of 5 μm thickness. The titanium(IV) oxide film was immersed in a solution, which contains dye (3×10^{-4} M), at ambient temperature for a day after the sintering process at 450°C followed by cooling (80°C). The solutions of N719-ruthenium complex (used as standard / reference) as well as all the new organic dyes were prepared in a mixture of solvents such as acetonitrile and 2-methylpropan-2-ol (1:1; v/v). The photoanode, dye-sensitized titanium(IV) oxide, thus equipped was kept on a conducting glass (sputtered; platinum) electrode, maintaining the couple of electrodes which are divided by a Surlyn® film (25 μm thick). Then, the couple of electrodes were sealed. The electrolyte - 0.1M LiI, 0.05 M I_2, 0.6M DMPII, 0.5M TBP, and in ACN and MPN solvent mixture (1:1 v/v).

In the counter electrode, a hole was made previously for the injection of electrolyte. Utilizing a capillary, the injection of electrolyte was done and after which it was sealed. The surface of the DSSCs was sheltered by a cover (0.16 cm^2 - light illuminated area) and subsequently it was illuminated by utilizing a solar simulator. Light-intensity (incident; 0.001 W / cm^2) was standardized with the help of a standard Si-cell. The width (thickness) of the titanium(IV) oxide film was evaluated using SEM. For recording UV-visible spectra, the dyes were layered on the titanium(IV) oxide films. The baseline was corrected using a naked

ACCEPTED MANUSCRIPT

titanium(IV) oxide coated FTO substrate. EIS were acquired from the potentiostat / galvanostat, prepared with an FRA2 module [light-illumination (constant); 0.001W / cm^2]. The range of frequency examined was 10–65 kHz. The voltage (applied bias) was set at the V_{oc} of the DSSC between the conducting glass–titanium(IV) oxide–dye working electrode and the indium tin oxide-platinum counter electrode, initiating from the short-circuit conditions; the equivalent AC amplitude was 10 mV. The analysis of EI spectra was made by an equivalent-circuit model. The curves of IPCE were acquired under short-circuit conditions. The source of light was a solar simulator (PEC-L11, class-A quality; AM 1.5G) and the light was focused - via a monochromator - on to the PV cell. The monochromator was added via visible-spectrum to produce the IPCE (λ). The J_{sc} (mA /cm^2) was measured with the help of a potentiostat-galvanostat, and the IRF (incident-radiative-flux (W/ m^2) was recorded with an OD (optical-detector) along with a power-meter.

3. Results and Discussion

3.1. Syntheses of metal free dyes

The synthetic strategy for building of novel title metal-free heterocyclic dyes **TBCPCA-1**, **TBCPCA-2**, **TBTCPCA-1** and **TBTCPCA-2** is provided in Scheme 1. N-tosylated intermediate **3** was synthesized from commercially available azafluorene **1** upon diiodination using potassium iodide and potassium iodate in acetic acid followed by tosylation with the help of *p*-toluenesulfonyl chloride in DMF. Besides, di-*tert*-butylated intermediate **4** was synthesized from azafluorene **1** through dialkylation utilizing *tert*-butyl chloride in nitromethane in the presence of zinc chloride. Ullmann type reaction between the intermediates **3** and **4** in the presence of cuprous oxide in N,N-dimethylacetamide furnished intermediate **5**, which upon

ACCEPTED MANUSCRIPT

detosylation with potassium hydroxide in aqueous tetrahydrofuran and N,N-dimethylformamide mixture gave intermediate **6**. On the other hand, bromo and carbaldehyde possessing fused thiazine intermediates **12** and **13** were synthesized from commercially available aryl fused thiazine **7** by employing alkylation using alkyl halide in dimethylsulfoxide followed by Vilsmeier-Haack and halogenation reactions. The Vilsmeier-Haack reaction was performed by employing phosphorous oxy chloride and N,N-dimethyl formamide in chloroform while the bromination reaction was carried out in acetic acid using bromine. The intermediates **12** and **13**, upon Ullmann type reaction with the previously synthesized intermediate **4** utilizing copper-bronze and potassium carbonate in *o*-dichlorobenzene under PTC (18-crown-6) furnished the carbaldehydes **14** and **15**, respectively, which upon subjected to Knoevenagel type reaction with cyanoacetic acid eventually provided the novel dyes **TBCPCA-1** and **TBCPCA-2**, respectively. Similarly, the intermediates **12** and **13**, upon Ullmann type condensation with the already synthesized intermediate **6** by employing copper-bronze and potassium carbonate in *o*-dichlorobenzene under PTC (18-crown-6) furnished the intermediates **16** and **17**, respectively which are further converted in to novel metal free fused heterocyclic dyes **TBTCPCA-1** and **TBTCPCA-2**, respectively through Knoevenagel type condensation. The structures of novel metal free fused heterocyclic dyes are established based on their physical and spectroscopic methods.

Scheme 1

3.2. Photophysical properties

Table 1

ACCEPTED MANUSCRIPT

The photo-physical properties of all the novel metal free heterocyclic dyes **TBCPCA-1**, **TBCPCA-2**, **TBTCPCA-1** and **TBTCPCA-2** are studied from the results of UV-Visible spectra recorded in dichloromethane and anchored on TiO_2 films. The spectra are furnished in Figure 3 and the subsequent data are provided Table 1. The absorption bands obtained from 250 nm to 375 nm are ascribed to localized π-π* electron transitions of the conjugated motif while the absorption bands resulted from 380 nm to 600 nm are due to strong ICT between the fused heterocyclic units and cycnoacrylic acid skeleton. Of the dyes, the one possessing di-*tert*-butylazafluorene structural motif at the 6-position of fused thiazine unit **(**i.e., **TBCPCA-1)** exhibited intramolecular charge transfer maximum at 456 nm, which is slightly higher than the one with tetra-*tert*-butyl-tri-(azafluorene) substituted analogue **TBTCPCA-1**. Similar trend is observed in the case of **TBCPCA-2** when compared with **TBTCPCA-2** though the difference in magnitude is comparatively higher. Normally, it is apparent that increasing conjugation in a molecule and / or assimilation of auxiliary electron releasing functional moieties provides the absorption maximum with bathochromic shift. Accordingly, the absorption maxima of the dyes possessing tetra-*tert*-butyl-tri-(azafluorene) structural motif such as **TBTCPCA-1** and **TBTCPCA-2** are expected to be in the bathochromic region when compared to the absorption maxima of the dyes having di-*tert*-butylazafluorene scaffold such as **TBCPCA-1** and **TBCPCA-2**. However, the obtained results are contrary to each other. The plausible rationale is the sterically crammed tetra-*tert*-butyl-tri-(azafluorene) structural motif in the dyes **TBTCPCA-1** and **TBTCPCA-2** increases the inter- and intramolecular aromatic-aromatic interactions between and with-in the dye molecules, respectively through edge-to-face (H-π) and / face-to-face interactions on comparing the dyes **TBCPCA-1** and **TBCPCA-2**, which possess less-sterically

ACCEPTED MANUSCRIPT

congested di-*tert*-butylazafluorene scaffold. Further, enhancing the bulkiness of a molecule generally decreases the dye-aggregation and consequently increases the molar extinction coefficient. This concept is realistic in our case as well since the molar extinction coefficient of the tetra-*tert*-butyl-tri-(azafluorene) scaffold containing dyes **TBTCPCA-1** and **TBTCPCA-2** are higher than that of the di-*tert*-butylazafluorene structural motif possessing dyes **TBCPCA-1** and **TBCPCA-2**. Amongst the dyes synthesized, **TBTCPCA-2** displayed the highest molar extinction coefficient. It was observed that the absorption maxima of the dyes are comparatively lower when they are adsorbed on TiO_2 films on comparing with the absorption of the respective dyes in dichloromethane solution. The absorption in the lower wavelength (hypsochromic shift) in the case of the former than the latter could be attributed to deprotonation on TiO_2 and / or H-aggregation for those dyes [53,72,73].

Figure 3

3.3. Electrochemical properties

In addition to the light collecting yield of nanocrystalline titania (dye-adsorbed), it is crucial that there are encouraging dye molecules energy off-sets with respect to the redox electrolyte and nanocrystalline titania in order to construct efficient DSSCs. Consequently, electrochemical activities of the novel heterocyclic dyes **TBCPCA-1**, **TBCPCA-2**, **TBTCPCA-1** and **TBTCPCA-2** were recorded with the help of cyclic voltametry in dichloromethane solution. The pictorial representations of the same are furnished in Figure 4 and the related data are given in Table 1. The dyes HOMO-LUMO level energies were recognized on evaluating the red-ox potentials of the heterocyclic dyes with oxidation potential of ferrocene. From the

ACCEPTED MANUSCRIPT

aforementioned data, the thermodynamic viability for injection of electron to the CB of nanocrystalline titania from the excited dye as well as the regeneration viability of the oxidized dyes by electrolyte were estimated.

Figure 4

Picture (energy level) exhibiting the oxidation potentials (GS and ES) for the novel fused heterocyclic dyes **TBCPCA-1**, **TBCPCA-2**, **TBTCPCA-1** and **TBTCPCA-2** is furnished in Figure 5. These potentials in the ground state range between 1.20 and 1.26V Vs NHE [74]. Among the dyes, the oxidation potentials of di-*tert*-butylazafluorene donor possessing ones **TBCPCA-1** and **TBCPCA-2** are relatively higher than that of the dyes containing tetra-*tert*-butyl-tri-(azafluorene) analogues **TBTCPCA-1** and **TBTCPCA-2**. Particularly, all the novel fused heterocyclic dyes exerted oxidation potential adequately positive compared to the red-ox potential of the electrolyte I^-/I_3^-, which is reported as 0.4V (Vs NHE), and has been frequently utilized in DSSCs. Thus, the oxidized fused heterocyclic dyes could ably be rejuvenated by the electrolyte I^-/I_3^-. At the same time, on comparing the first oxidation potential of the dyes **TBCPCA-1**, **TBCPCA-2**, **TBTCPCA-1** and **TBTCPCA-2** with the conduction band edge of nanocrystalline titania semiconductor, the former ones exhibit sufficiently negative than the latter as the first oxidation potential of the former (i.e., dyes) lies between 1.19 and -1.35V while the latter (i.e., semiconductor) reported to be -0.5V (Vs NHE). Specifically, the potential difference between the fused heterocyclic dyes and the CB edge of nanocrystalline titania is greater than 0.69V and this difference in potential is ample to give the thermodynamic feasibility for the electrons injection to the CB of nanocrystalline titania from the excited dyes [27]. The oxidation

ACCEPTED MANUSCRIPT

potential results of ground and excited states of all the fused heterocyclic dyes imply that these are estimated to serve as capable sensitizers in nanocrystalline titania based DSSCs.

Figure 5

3.4. Computational approaches

DFT calculations were performed to acquire further information regarding molecular structure and electronic sharing of the FMO of the fused heterocyclic dyes **TBCPCA-1, TBCPCA-2, TBTCPCA-1** and **TBTCPCA-2** [75-77]. For the optimization of the chemical structures of all the new heterocyclic dye molecules, DFT-B3LYP (Becke3 Lee-Yang-Parr) method with 6-311++G(d,p) basis set using Gaussian 09 program package was used. The FMOs of the heterocyclic dyes at the aforesaid level are provided in Figure 6.

Figure 6

The density of electrons in the HOMO level of the dyes **TBTCPCA-1** and **TBTCPCA-2** is mainly distributed on the fused thiazine scaffold whereas the electron density in the LUMO level of the same is localized precisely on the cyanoacrylic acid segment. Similar trend is observed in the cases of **TBCPCA-1** and **TBCPCA-2** wherein the distribution of electrons in the homo level is on the fused thiazne structural motif while the the same in lumo level is on the cyanoacrylic acid unit. As an overall observation, it is apparent that the excitation of electrons from HOMO to LUMO by light induces facile shift of the electrons from fused thiazine structural moiety to cyanoacrylic acid scaffold in the cases of **TBTCPCA-1**, **TBTCPCA-2**,

ACCEPTED MANUSCRIPT

TBCPCA-1 and **TBCPCA-2**. Consequently, the aforementioned trend in the distribution of electrons makes us to speculate that the electrons which are excited could adequately be injected in-to the conduction band of nanocrystalline titania via the cyanoacrylic acid acceptor moiety. It is well recognized that a charge transfer in a facile manner could avoid come into existence of recombination of charge between dye molecules (oxidized) and photo-induced electrons at the semiconductor/dye/electrolyte interface [78]. As can be seen in the Figure 6, the thiazine structural motif is non-planar and puckered conformation with an equatorial disposition of alkyl substituent; as a result, it restrains the aggregation because the aforementioned conformation exposes the character of non-aromatic of the fused thiazine motif, which could decrease the π-π stacking between the molecules of the dye [61].

3.5. Photovoltaic performance

Table 2

Fabrication of DSSCs was made using all the four heterocyclic dyes **TBCPCA-1**, **TBCPCA-2**, **TBTCPCA-1** and **TBTCPCA-2** as sensitizers on titania films in combination with the liquid electrolytic system and the photovoltaic parameters of the fabricated cells were acquired under irradiation at standard AM 1.5G. The noteworthy parameters of the DSSCs (*ff*, J_{sc}, V_{oc}, and η) are furnished in Table 2. The *J-V* uniqueness of the DSSCs (solar irradiation at AM 1.5G), are given in Figure 7.

Figure 7

ACCEPTED MANUSCRIPT

The dye-sensitized solar cell possessing **TBCPCA-2** sensitizer exhibited the highest photocurrent while the ones possessing **TBCPCA-2** and **TBTCPCA-2** sensitizers showed the highest open-circuit voltage. On comparing the fused heterocyclic dyes containing di-*tert*-butylazafluorene structural unit as an electron donor (**TBCPCA-1** and **TBCPCA-2)**, the ones comprising tetra-*tert*-butyl-tri-(azafluorene) scaffold as the same **(TBTCPCA-1** and **TBTCPCA-2)** ended-up with lower photo-current density. The bulkier tetra-*tert*-butyl-tri-(azafluorene) scaffold of the dyes **TBTCPCA-1** and **TBTCPCA-2** might probably have reduced the dye loading on the nanocrystalline titania semiconductor surface and consequently light harvesting tendency and thus culminated with the aforementioned lower photo-current density. The low photocurrent density may occur due to poor contact between the nanocrystalline titania semiconductor and the dye due to the presence of additional couple of bulky azafluorene structural units. In addition, on comparing the dyes having di-*tert*-butylazafluorene scaffold as donor **(**i.e., **TBCPCA-1** and **TBCPCA-2)**, the dyes possessing tetra-*tert*-butyl-tri-(azafluorene) unit as the same **(**i.e., **TBTCPCA-1** and **TBTCPCA-2)** exhibit larger dark current. This increasing fashion of dark current from the former type of dyes to the latter ones implies that the former ones are more capable to reduce electron leakage than the latter ones. Normally, this could be understood with no doubt since on contrast to the molecules with larger in size which build efficient barriers that hinders the approach of I_3^- towards the surface of nanocrystalline titania, molecules with smaller in size are prone to form tightly packed monolayer as a consequence of smaller amount of steric interruption.

ACCEPTED MANUSCRIPT

IPCE appraised alongside the wavelength of irradiation for the dye sensitized solar cells possessing the dyes **TBCPCA-1, TBCPCA-2, TBTCPCA-1** and **TBTCPCA-2** as sensitizers are provided in Figure 8. All the aforementioned dyes demonstrated conversion efficiency of photon-to-electron between 400 to 750 nm wavelength. Particularly, the dyes **TBCPCA-1, TBCPCA-2** and **TBTCPCA-1** exerted high IPCE between 400 to 650 nm while the dye **TBTCPCA-2** displayed slightly lower IPCE compared to the others. Of all, the dye **TBCPCA-2** showed the highest IPCE (80 to >95%). Further, all the dyes displayed power conversion efficiencies between 6.17 and 7.97%. On comparing the power conversion efficiencies between the dyes possessing di-*tert*-butylazafluorene structural motif as electron donor (i.e., **TBCPCA-1** and **TBCPCA-2**) and the ones containing tetra-*tert*-butyl-tri-(azafluorene) scaffold as electron donor (i.e., **TBTCPCA-1** and **TBTCPCA-2**), the former category of dyes provided higher efficiencies than the latter category of dyes. Among all the devices fabricated, the device with the utilization of **TBCPCA-2** as a sensitizer exhibited highest power conversion efficiency. This highest efficiency initiated from the photo current density distinction when compared to others. The higher IPCE and photo-current density values resulted for the DSSC with the **TBCPCA-2** as the sensitizer are trustworthy with the property of absorption [79-81]. The device with the employment of the dye **TBCPCA-2** as a sensitizer showed a *ff* of 0.67±0.003, a V_{oc} of 745±0.6 mV, a J_{sc} of 16.92±0.3 mA cm^{-2}, and PCE (η) of 7.97±0.3%, which is the highest one when compared to the devices fabricated with the utilization of the other dyes **TBCPCA-1, TBTCPCA-1** and **TBTCPCA-2** as sensitizers.

Figure 8

ACCEPTED MANUSCRIPT

3.6. Electrochemical impedance spectroscopy

It is documented that as a consequence of electrons in comparatively huge quantity in the nanocrystalline titania conduction band, high open-circuit voltage could be observed. The solidity of electrons in the conduction band of nanocrystalline titania may be a result of enhanced efficiency of charge collection in the equivalent dye-sensitized solar cell device. Therefore, EI spectra were acquired (illumination - 100 $mW.cm^{-2}$) to explore the relative charge-collection rate in the DSSC devices with the dyes **TBCPCA-1, TBCPCA-2, TBTCPCA-1** and **TBTCPCA-2**. As can be seen in Figure 9 (equivalent circuit 9a), reasonably large middle semicircles were obtained in the Nyquist plot, measured under standard illumination conditions for the new metal free heterocyclic dyes **TBCPCA-1, TBCPCA-2, TBTCPCA-1** and **TBTCPCA-2**. The resulted semicircles suggest a huge electron transport resistance for their devices in the series and the order is furnished herein: **TBTCPCA-2** > **TBTCPCA-1** > **TBCPCA-1** > **TBCPCA-2**. The small electron transport resistance for the dye **TBCPCA-2** over **TBCPCA-1, TBTCPCA-1** and **TBTCPCA-2** proposes enhanced efficiency of electron collection of the former compared to the latter. A careful observation between the electron transport resistance and the power conversion efficiency implies that the dye with low electron transport resistance showed higher power conversion efficiency and hence there is a fine relationship between the same. Further, the devices directed to superior photocurrent due to the enhanced efficiency of electron collection. Therefore, the improved performance of the dye **TBCPCA-2** over the other heterocyclic dyes viz., **TBCPCA-1, TBTCPCA-1** and **TBTCPCA-2** may be credited to the superior electron-gathering supported by the encouraging electron-releasing in the **TBCPCA-2**. Further, the R_{Ct2} at the interface of nanocrystalline titania-dye-electrolyte is lesser in the case of DSSC with the dye **TBCPCA-2** as sensitizer relative to the DSSCs with the dyes **TBCPCA-1, TBTCPCA-1** and

ACCEPTED MANUSCRIPT

TBTCPCA-2 as sensitizers (Table 2), implies an effective electron collection for the device with the dye **TBCPCA-2**. This observation is in harmony with the superior values of short-circuit current resulted for the device with the dye **TBCPCA-2**.

Figure 9

Additionally, DSSCs Bode-phase plots were measured under conditions of illumination to judge the life time of electron within the semiconductor (τ_e). The pictorial representation of the same is furnished in Figure 10. The frequency of the peaks resulted in the region of middle-frequency can be used to judge the same. This provides a further suggestion of the rate of charge recombination. The results of electron life time are reliable with the results of V_{oc}. The definite order of open-circuit voltage as well as electron life time for the novel heterocyclic dyes is **TBCPCA-2 ≈ TBTCPCA-2 > TBTCPCA-1 > TBCPCA-1**. In order to determine the efficiency of DSSCs, there are a couple of processes that can participate in an imperative role: (i) aggregation of dye and (ii) injected electrons recombination process on nanocrytalline titania semiconductor with the electrolyte and / or oxidized dye. Conversely, the aforementioned processes are also controlled by the bonding between the dye and nanocrystalline titania, the energy disparity between the conduction band of nanocrystalline titania and the dye's excited state and the dye rejuvenation by the redox electrolyte. It is recognized that the degree of the move of CB commonly rely on the nanocrystalline titania semiconductor /dye interfacial-dipole which, further is affected by the electronic blending between the nanocrystalline titania semiconductor and the dye.

ACCEPTED MANUSCRIPT

Figure 10

The resulted high J_{sc} of 16.92±0.3 mA.cm^{-2} for the DSSC with **TBCPCA-2** as a sensitizer could be owing to the finer electronic interaction of the dye with the nanocrystalline titania semiconductor. Usually, electrochemical impedance spectrum of a FTO/TiO_2/dye/electrolyte/Pt/ITO device exhibits three semicircles between 10 mHz to 65 kHz. The R_S is for the overall series resistance. The first semicircle is for the CT resistance at the counter-electrode (R_{Ct1}) while the second and third ones are for the semiconductor/dye/electrolyte interface (R_{Ct2}) and the Warburg diffusion method of I^-/I_3^- in the electrolyte (Z_w), respectively. On the other hand, in our study, the predictable diffusion resistance of the redox couple is in fact considerably overlapped by R_{Ct2} because of a undersized length for the diffusion of I^- ion available with the 25 μm thin spacer utilized, and because of the exploitation of low viscosity solvents in our electrolyte (viscosities of MPN and ACN are 1.60 cp and 0.37 cp, respectively).

4. Conclusions

A series of azafluorene ornamented thiazine based novel fused heterocyclic organic dyes **TBCPCA-1, TBCPCA-2, TBTCPCA-1** and **TBTCPCA-2** has been synthesized by adopting a multi-step synthetic strategy. The dyes **TBCPCA-1** and **TBCPCA-2** possessing di-*tert*-butylazafluorene structural motif as an electron donor showed comparatively higher power conversion efficiencies over the dyes **TBTCPCA-1** and **TBTCPCA-2** containing sterically congested tetra-*tert*-butyl-tri-(azafluorene) scaffold as an electron donor. Amongst the devices fabricated with the utilization of novel dyes, the **TBCPCA-2** carrying device exhibited the

ACCEPTED MANUSCRIPT

highest power conversion efficiency of 7.97±0.3% along with the IPCE of 80 to >95%. In the energy levels of HOMO-LUMO of all the novel heterocyclic dyes, well separated distribution of electrons has been observed; imply ample release of excited electrons to the CB of the semiconductor via carboxylic acid structural motif. Further, the elevated short-circuit current and inferior CT resistance at the nanocrystalline titania/dye/electrolyte interface observed in **TBCPCA-2** possessing dye sensitized solar cell support the superior electronic interaction of the nanocrystalline titania semiconductor with the dye and an effective electron collection for the device, respectively. Attention towards the modification of donor and acceptor scaffolds so as to improve the PCE further is under the way.

Acknowledgements

Financial assistance provided by the Department of Science and Technology (DST-SERB), New Delhi, India under Fast-Track Scheme (SR/FT/CS-149/2011) and the Ministry of Science and Technology of Taiwan (MOST-102-2221-E-002-186-MY3) are gratefully acknowledged.

ACCEPTED MANUSCRIPT

References

[1] Y. Bai, I. Mora-Sero, F. De Angelis, J. Bisquert, P. Wang, Titanium dioxide nanomaterials for photovoltaic applications, Chem. Rev. 114 (2014) 10095-10130.

[2] J. Wang, K. Liu, L. Ma, X. Zhan, Triarylamine: versatile platform for organic, dye-sensitized, and perovskite solar cells, Chem. Rev. 116 (2016) 14675-14725.

[3] L. -L. Li, E. W. -G Diau, Porphyrin-sensitized solar cells, Chem. Soc. Rev. 42 (2013) 291-304.

[4] B. Pashaei, H. Shahroosvand, M. Grätzel, M. K. Nazeeruddin, Influence of ancillary ligands in dye-sensitized solar cells, Chem. Rev. 116 (2016) 9485-9564.

[5] C. -P. Lee, R. Y. -Y. Lin, L. -Y. Lin, C. -T. Li, T. -C. Chu, S. -S. Sun, J. -T. Lin, K. -C. Ho, Recent progress in organic sensitizers for dye-sensitized solar cells, RSC Adv. 5 (2015) 23810-23825.

[6] F. Bella, C. Gerbaldi, C. Barolo, M. Grätzel, Aqueous dye-sensitized solar cells, Chem. Soc. Rev. 44 (2015) 3431-3473.

[7] A. Yella, H. -W. Lee, H. N. Tsao, C. Yi, A. K. Chandiran, M. K. Nazeeruddin, E. W. -G. Diau, C. -Y. Yeh, S. M. Zakeeruddin, M. Grätzel, Porphyrin-sensitized solar cells with cobalt (II/III)–based redox electrolyte exceed 12 % efficiency, Science 334 (2011) 629-634.

[8] M. Grätzel, Solar energy conversion by dye-sensitized photovoltaic cells, Inorg. Chem. 44 (2005) 6841-6851.

[9] B. O'Regan, M. Grätzel, A low-cost, high-efficiency solar cell based on dye-sensitized colloidal TiO_2 films, Nature 353 (1991) 737-740.

ACCEPTED MANUSCRIPT

[10] A. Yella, C. -L. Mai, S. M. Zakeeruddin, S. -N. Chang, C. -H. Hsieh, C. -Y. Yeh, M. Grätzel, Molecular engineering of push-pull porphyrin dyes for highly efficient dye-sensitized solar cells: the role of benzene spacers, Angew. Chem. Int. Ed. 53 (2014) 2973-2977.

[11] M. J. Griffith, K. Sunahara, P. Wagner, K. Wagner, G. Wallace, D. L. Officer, A. Furube, R. Katoh, S. Mori, A. J. Mozer, Porphyrins for dye-sensitised solar cells: new insights into efficiency-determining electron transfer steps, Chem. Commun. 48 (2012) 4145-4162.

[12] C. -Y. Chen, M. Wang, J. -Y. Li, N. Pootrakulchote, C. N. Alibabaei, J. -D. Decoppet, J. -H. Tsai, C. Grätzel, C. -G. Wu, S. M. Zakeeruddin, M. Grätzel, Highly efficient light-harvesting ruthenium sensitizer for thin-film dye-sensitized solar cells, ACS Nano 3 (2009) 3103-3109.

[13] M. Urbani, M. Gratzel, M. K. Nazeeruddin, T. Torres, Meso-substituted porphyrins for dye-sensitized solar cells, Chem. Rev. 114 (2014) 12330-12396.

[14] P. Wang, C. Klein, R. Humphry-Baker, S. M. Zakeeruddin, M. Grätzel, A high molar extinction coefficient sensitizer for stable dye-sensitized solar cells, J. Am. Chem. Soc. 127 (2005) 808-809.

[15] P. Wang, S. M. Zakeeruddin, J. -E. Moser, M. K. Nazeeruddin, T. Sekiguchi, M. Grätzel, A stable quasi-solid-state dye-sensitized solar cell with an amphiphilic ruthenium sensitizer and polymer gel electrolyte, Nat. Mater. 2 (2003) 402-407.

[16] D. Kuang, C. Klein, S. Ito, J. -E. Moser, R. Humphry-Baker, N. Evans, F. Duriaux, C. Grätzel, S. M. Zakeeruddin, M. Grätzel, High-efficiency and stable mesoscopic dye-sensitized solar cells based on a high molar extinction coefficient ruthenium sensitizer and nonvolatile electrolyte, Adv. Mater. 19 (2007) 1133-1137.

[17] F. Gao, Y. Wang, D. Shi, J. Zhang, M. Wang, X. Jing, R. Humphry-Baker, P. Wang, S. M. Zakeeruddin, M. Grätzel, Enhance the optical absorptivity of nanocrystalline TiO_2 film with

ACCEPTED MANUSCRIPT

high molar extinction coefficient ruthenium sensitizers for high performance dye-sensitized solar cells, J. Am. Chem. Soc. 130 (2008) 10720-10728.

[18] S. Mathew, A. Yella, P. Gao, R. Humphry-Baker, B. F. E. Curchod, N. Ashari-Astani, I. Tavernelli, U. Rothlisberger, M. K. Nazeeruddin, M. Grätzel, Dye-sensitized solar cells with 13% efficiency achieved through the molecular engineering of porphyrin sensitizers, Nat. Chem. 6 (2014) 242-247.

[19] T. Bessho, S. M. Zakeeruddin, C. -Y. Yeh, E. W. -G. Diau, M. Grätzel, Highly efficient mesoscopic dye-sensitized solar cells based on donor–acceptor-substituted porphyrins, Angew. Chem. Int. Ed. 49 (2010) 6646-6649.

[20] H.-H. Gao, X. Qian, W.-Y. Chang, S.-S. Wang, Y.-Z. Zhu, J.-Y. Zheng, Oligothiophene-linked D–π–A type phenothiazine dyes for dye-sensitized solar cells, J. Power Sources 307 (2016) 866-874.

[21] T. Li, J. Gao, Y. Cui, C. Zhong, Q. Ye, L. Han, Novel D-π-A carbazole sensitizers with 4-phenyl-2-(thiophen-2-yl)thiazole as π-bridge for dye-sensitized solar cells, J. Photochem. Photobiol. A 303 (2015) 91-98.

[22] C. Li, M. Liu, N. G. Pschirer, M. Baumgarten, K. Mullen, Polyphenylene-Based Materials for Organic Photovoltaics, Chem. Rev. 110 (2010) 6817-6855.

[23] A. Mishra, M. K. R. Fischer, P. Bauerle, Metal-free organic dyes for dye-sensitized solar cells: from structure: property relationships to design rules, Angew. Chem. Int. Ed. 48 (2009) 2474-2499.

[24] J.-F. Huang, J.-M. Liu, L.-L. Tan, Y.-F. Chen, Y. Shen, L.-M. Xiao, D.-B. Kuang, C.-Y. Su, Novel carbazole based sensitizers for efficient dye-sensitized solar cells: Role of the hexyl chain, Dyes and Pigments 114 (2015) 18-23.

ACCEPTED MANUSCRIPT

[25] E. M. Barea, J. Bisquert, Properties of chromophores determining recombination at the TiO_2–dye–electrolyte interface, Langmuir 29 (2013) 8773-8781.

[26] A. Mishra, C.-Q. Ma, P. Bauerle, Functional oligothiophenes: molecular design for multidimensional nanoarchitectures and their applications, Chem. Rev. 109 (2009) 1141-1276.

[27] Hagfeldt, G. Boschloo, L. Sun, L. Kloo, H. Pettersson, Dye-sensitized solar cells, Chem. Rev. 110 (2010) 6595-6663.

[28] Y. Ooyama, Y. Harima, Photophysical and electrochemical properties, and molecular structures of organic dyes for dye-sensitized solar cells, ChemPhysChem. 13 (2012) 4032-4080.

[29] S. Haid, M. Marszalek, A. Mishra, M. Wielopolski, T. Joel, J. E. Moser, R. Humphry-baker, S. M. Zakeeruddin, M. Gratzel, P. Bauerle, Significant improvement of dye-sensitized solar cell performance by small structural modification in π-conjugated donor–acceptor dyes, Adv. Funct. Mater. 22 (2012) 1291-1302.

[30] M. Liang, J. Chen, Arylamine organic dyes for dye-sensitized solar cells, Chem. Soc. Rev. 42 (2013) 3453-3488.

[31] G. Kim, K. Chung, J. Kim, Molecular design principle of all-organic dyes for dye-sensitized solar cells, Chem. Eur. J. 19 (2013) 5220-5230.

[32] Y. Z. Wu, W. H. Zhu, Organic sensitizers from D–π–A to D–A–π–A: effect of the internal electron-withdrawing units on molecular absorption, energy levels and photovoltaic performances, Chem. Soc. Rev. 42 (2013) 2039-2058.

[33] Y. S. Yen, H. H. Chou, Y. C. Chen, C. Y. Hsu, J. T. Lin, Recent developments in molecule-based organic materials for dye-sensitized solar cells, J. Mater. Chem. 22 (2012) 8734-8747.

ACCEPTED MANUSCRIPT

[34] Y. Cui, Y. Wu, X. Lu, X. Zhang, G. Zhou, F. B. Miapeh, W. Zhu, Z.-S. Wang, Incorporating benzotriazole moiety to construct D–A−π–A organic sensitizers for solar cells: significant enhancement of open-circuit photovoltage with long alkyl group, Chem. Mater. 23 (2011) 4394-4401.

[35] X. Hu, S. Cai, G. Tian, X. Li, J. Su, J. Li, Rigid triarylamine-based D–A–π–A structural organic sensitizers for solar cells: the significant enhancement of open-circuit photovoltage with a long alkyl group, RSC Adv. 3 (2013) 22544-22553.

[36] N. Koumura, Z.-S. Wang, S. Mori, M. Miyashita, E. Suzuki, K. Hara, Alkyl-functionalized organic dyes for efficient molecular photovoltaics, J. Am. Chem. Soc. 128 (2006) 14256-14257.

[37] Z. Wang, N. Koumura, Y. Cui, M. Takahashi, H. Sekiguchi, A. Mori, T. Kubo, A. Furube, K. Hara, Hexylthiophene-functionalized carbazole dyes for efficient molecular photovoltaics: tuning of solar-cell performance by structural modification, Chem. Mater. 20 (2008) 3993-4003.

[38] Z. Yao, M. Zhang, H. Wu, L. Yang, R. Li, P. Wang, Donor/acceptor indenoperylene dye for highly efficient organic dye-sensitized solar cells, J. Am. Chem. Soc. 137 (2015) 3799-3802.

[39] K. Kakiage, Y. Aoyama, T. Yano, T. Otsuka, T. Kyomen, Unno, M. Hanaya, An achievement of over 12 percent efficiency in an organic dye-sensitized solar cell, Chem. Commun. 50 (2014) 6379-6381.

[40] M. Zhang, Y. Wang, M. Xu, W. Ma, R. Li, P. Wang, Design of high-efficiency organic dyes for titania solar cells based on the chromophoric core of cyclopentadithiophene-benzothiadiazole, Energy Environ. Sci. 6 (2013) 2944-2949.

ACCEPTED MANUSCRIPT

[41] G. Zhang, H. Bala, Y. Cheng, D. Shi, X. Lv, Q. Yu, P. Wang, High efficiency and stable dye-sensitized solar cells with an organic chromophore featuring a binary π-conjugated spacer, Chem. Commun. (2009) 2198-2200.

[42] D. Tavgeniene, J. V. Grazulevicius, L. Liu, G. Krucaite, Z. Xie, B. Zhang, D. Volyniuk, S. Grigalevicius, Phenylvinyl-substituted carbazole twin compounds as efficient materials for the charge-transporting layers of OLED devices, J. Electron. Mater. 44 (2015) 4006-4011.

[43] L. Shi, Z. Liu, W. Guo, G. Dong, D. Zhao, L. Duan, D. Cui, Y. Qiu, X. Tao, J. Jia, Synthesis, structure, properties, and application of a carbazole-based diaza[7]helicene in a deep-blue-emitting OLED, Chem. Eur. J. 18 (2012) 8092-8099.

[44] J. K. Salunke, F. L. Wong, K. Feron, S. Manzhos, M. F. Lo, D. Shinde, A. Patil, C. S. Lee, V. A. L. Roy, P. Sonar, P. P. Wadgaonkar, Phenothiazine and carbazole substituted pyrene based electroluminescent organic semiconductors for OLED devices, J. Mater. Chem. C 4 (2016) 1009-1018.

[45] S. Soman, M. A. Rahim, S. Lingamoorthy, C. H. Suresh, S. Das, Strategies for optimizing the performance of carbazole thiophene appended unsymmetrical squaraine dyes for dye-sensitized solar cells, Phys. Chem. Chem. Phys. 17 (2015) 23095-23103.

[46] M. Tavasli, V. Jankus, T. N. Moore, H. A. Al-Attar, Y. Zheng, M. R. Bryce, A. P. Monkman, M. A. Fox, G. C. Griffiths, Colour tuning from green to red by substituent effects in phosphorescent tris-cyclometalated iridium(III) complexes of carbazole-based ligands: synthetic, photophysical, computational and high efficiency OLED studies, J. Mater. Chem. 22 (2012) 6419-6428.

ACCEPTED MANUSCRIPT

[47] S. S. Soni, K. B. Adadu, J. V. Vaghasiya, B. G. Solanki, K. K. Sonigara, A. Singh, D. Das, P. K. Iyer, Improved molecular architecture of D–π–A carbazole dyes: 9% PCE with a cobalt redox shuttle in dye sensitized solar cells, J. Mater. Chem. A 3 (2015) 21664-21671.

[48] K. R. J. Thomas, A. Venkateswararao, C. -P. Lee, K. -C. Ho, Organic dyes containing fluoreneamine donor and carbazole π-linker for dye-sensitized solar cells, Dyes and Pigments 123 (2015) 154-165.

[49] X. Qian, Y -Z. Zhu, W -Y. Chang, J. Song, B. Pan, L. Lu, H. -H. Gao, J. -Y. Zheng, Benzo[a]carbazole-based donor-π-acceptor type organic dyes for highly efficient dye-sensitized solar cells, ACS Appl. Mater. Interfaces 7 (2015) 9015-9022.

[50] W. Cao, M. Fang, Z. Chai, H. Xu, T. Duan, Z. Li, X. Chen, J. Qina, H. Han, New D–π–A organic dyes containing a tert-butyl-capped indolo[3,2,1-jk]carbazole donor with bithiophene unit as π-linker for dye-sensitized solar cells, RSC Adv. 5 (2015) 32967-32975.

[51] L -L, Tan, J. -F. Huang, Y. Shen, L. -M. Xiao, J. -M. Liu, D. -B. Kuanga, C. -Y. Su, Highly efficient and stable organic sensitizers with duplex starburst triphenylamine and carbazole donors for liquid and quasi-solid-state dye-sensitized solar cells, J. Mater. Chem. A 2 (2014) 8988-8994.

[52] K. Lim, K. Song, Y. Kang, J. Ko, Organic sensitizers possessing carbazole donor and indeno[1,2-b] thiophene spacer for efficient dye sensitized solar cells, Dyes and Pigments 119 (2015) 41-48.

[53] A. Venkateswararao, K. R. J. Thomas, C. -P. Lee, C. -T. Li, K. -C. Ho, Organic dyes containing carbazole as donor and π-linker: optical, electrochemical, and photovoltaic properties, ACS Appl. Mater. Interfaces 6 (2014) 2528-2539.

ACCEPTED MANUSCRIPT

[54] L. Zhao, P. Wagner, A. B. S. Elliott, M. J. Griffith, T. M. Clarke, K. C. Gordon, S. Moric, A. J. Mozer, Enhanced performance of dye-sensitized solar cells using carbazole-substituted di-chromophoric porphyrin dyes, J. Mater. Chem. A 2 (2014) 16963-16977.

[55] Y. Uemura, T. N. Murakami, N. Koumura, Crown ether-substituted carbazole dye for dye-sensitized solar cells: controlling the local ion concentration at the TiO_2/dye/electrolyte interface, J. Phys. Chem. C 118 (2014) 16749-16759.

[56] A. Venkateswararao, K. R. J. Thomas, Solar Cell Nanotechnology (2014) 41-96, Atul Tiwari, Rabah Boukherroub, Maheshwar Sharon (eds.), Scrivener Publishing LLC and references cited therein.

[57] Y. Hua, S. Chang, J. He, C. Zhang, J. Zhao, T. Chen, W. -Y. Wong, W. -K. Wong, X. Zhu, Molecular engineering of simple phenothiazine-based dyes to modulate dye aggregation, charge recombination, and dye regeneration in highly efficient dye-sensitized solar cells, Chem. Eur. J. 20 (2014) 6300-6308.

[58] W. J. Wu, J. B. Yang, J. L. Hua, J. Tang, L. Zhang, Y. T. Long, H. Tian, Efficient and stable dye-sensitized solar cells based on phenothiazine sensitizers with thiophene units, J. Mater. Chem. 20 (2010) 1772-1779.

[59] R. -Y. Lin, T. -M. Chuang, F. -L. Wu, P. -Y. Chen, T. -C. Chu, J. -S. Ni, M. -S. Fan, Y. -H. Lo, K. -C. Ho, J. T. Lin, Anthracene/phenothiazine π-conjugated sensitizers for dye-sensitized solar cells using redox mediator in organic and water-based solvents, ChemSusChem. 8 (2015) 105-113.

[60] X. Liu, J. Long, G. Wang, Y. Pei, B. Zhao, S. Tan, Effect of structural modification on the performances of phenothiazine-dye sensitized solar cells, Dyes and Pigments 121 (2015) 118-127.

ACCEPTED MANUSCRIPT

[61] H. Tian, X. C. Yang, R. K. Chen, Y. Z. Pan, L. Li, A. Hagfeldt, L. C. Sun, Phenothiazine derivatives for efficient organic dye-sensitized solar cells, Chem. Commun. (2007) 3741-3743.

[62] C.-J. Yang, Y.J. Chang, M. Watanabe, Y.-S. Hon, T. J. Chow, Phenothiazine derivatives as organic sensitizers for highly efficient dye-sensitized solar cells, J. Mater. Chem. 22 (2012) 4040-4049.

[63] M.-J. Kim, Y.-J. Yu, J.-H. Kim, Y.-S. Jung, K.-Y. Kay, S.-B. Ko, C.-R. Lee, I.-H. Jang, Y.-U. Kwon, N.-G. Park, Tuning of spacer groups in organic dyes for efficient inhibition of charge recombination in dye-sensitized solar cells, Dyes and pigments 95 (2012) 134-141.

[64] S. Wang, H. Wang, J. Guo, H. Tang, J. Zhao, Influence of the terminal electron donor in D-D-π-A phenothiazine dyes for dye-sensitized solar cells, Dyes and pigments 109 (2014) 96-104.

[65] K. Brunner, A. Van Dijken, H. Börner, J. J. A. M. Bastiaansen, N. M. M. Kiggen, B. M. W. Langeveld, Carbazole compounds as host materials for triplet emitters in organic light - emitting diodes: tuning the HOMO level without influencing the triplet energy in small molecules, J. Am. Chem. Soc. 126 (2004) 6035-6042.

[66] J. H. Yum, D. P. Hagberg, S. J. Moon, K. M. Karlsson, T. Marinado, L. C. Sun, A. Hagfeldt, M. K. Nazeeruddin, M. Gratzel, A light-resistant organic sensitizer for solar-cell applications, Angew. Chem. Int. Ed. 48 (2009) 1576-1580.

[67] C. Teng, X. Yang, S. Li, M. Cheng, A. Hagfeldt, L. Wu, L. C. Sun, Tuning the HOMO energy levels of organic dyes for dye-sensitized solar cells based on Br^-/Br_3^- electrolytes, Chem. Eur. J. 16 (2010) 13127-13138.

ACCEPTED MANUSCRIPT

[68] W. Lee, N. Cho, J. Kwon, J. Ko, J. I. Hong, New organic dye based on a 3,6-disubstituted carbazole donor for efficient dye-sensitized solar cells, Chem. Asian J. 7 (2012) 343-350.

[69] S. H. Kim, C. Sakong, J. B. Chang, B. Kim, M. J. Ko, D. H. Kim, K. S. Hong, J. P. Kim, The effect of N-substitution and ethylthio substitution on the performance of phenothiazine donors in dye-sensitized solar cells, Dyes and Pigments 97 (2013) 262-271.

[70]X. Yang, R. Lu, F. Gai, P. Xue, Y. Zhan. Rigid dendritic gelators based on oligocarbazoles, Chem. Commun. 46 (2010) 1088-1090.

[71] Y. Liu, M. Nishiura, Y. Wang, Z. Hou. π-Conjugated aromatic enynes as a single-emitting component for white electroluminescence, J. Am. Chem. Soc. 128 (2006) 5592-5593.

[72] K. Sayama, S. Tsukagoshi, K. Hara, Y. Ohga, A. Shinpou, Y. Abe, S. Suga, H. Arakawa, Photoelectrochemical properties of *J* aggregates of benzothiazole merocyanine dyes on a nanostructured TiO_2 film, J. Phys. Chem. B 106 (2002) 1363-1371.

[73] C. Teng, X. Yang, C. Yang, H. Tian, S. Li, X. Wang, A. Hagfeldt, L. Sun, Influence of triple bonds as π-spacer units in metal-free organic dyes for dye-sensitized solar cells, J. Phys. Chem. C 114 (2010) 11305-11313.

[74] M. Gratzel, Photoelectrochemical cells, Nature 414 (2001) 338-344.

[75] R. G. Parr, W. Yang, Density-functional theory of the electronic structure of molecules, Annu. Rev. Phys. Chem. 46 (1995) 701-728.

[76] C. Lee, W. Yang, R. G. Parr, Development of the Colle-Salvetti correlation-energy formula into a functional of the electron density, Phys. Rev. B: Condens. Matter. Phys. 37 (1988) 785-789.

[77] A. D. Becke, A new mixing of Hartree–Fock and local density-functional theories, J. Chem. Phys. 98 (1993) 1372.

ACCEPTED MANUSCRIPT

[78] W. D. Zeng, Y. M. Cao, Y. Bai, Y. H. Wang, Y. S. Shi, M. Zhang, F. F. Wang, C. Y. Pan, P. Wang, Efficient dye-sensitized solar cells with an organic photosensitizer featuring orderly conjugated ethylenedioxythiophene and dithienosilole blocks, Chem. Mater. 22 (2010) 1915-1925.

[79] S. Kim, J. K. Lee, S. O. Kang, J. Ko, J. H. Yum, S. Fantacci, F. D. Angelis, D. D. Censo, M. K. Nazeeruddin, M. Gratzel, Molecular engineering of organic sensitizers for solar cell applications, J. Am. Chem. Soc. 128 (2006) 16701-16707.

[80] C. O'Rourke, D. R. Bowler, Adsorption of thiophene-conjugated sensitizers on TiO_2 anatase (101), J. Phys. Chem. C 114 (2010) 20240-20248.

[81] D. Kumar, K. R. J. Thomas, C. -P. Lee, K. -C. Ho, Organic dyes containing fluorene decorated with imidazole units for dye-sensitized solar cells, J. Org. Chem. 79 (2014) 3159-3172.

ACCEPTED MANUSCRIPT

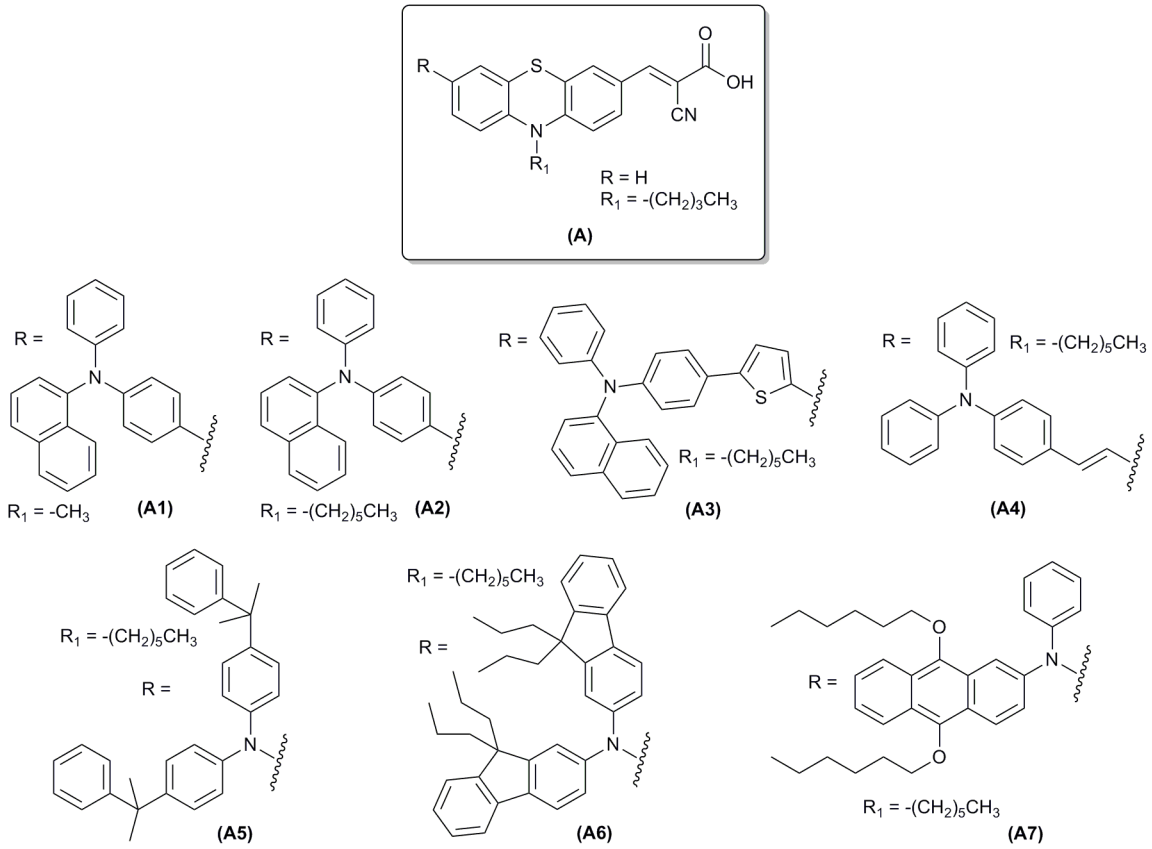

Figure 1. Structures of reported thiazine based fused heterocyclic dyes possessing amino and cyanoacrylic acid structural motifs.

ACCEPTED MANUSCRIPT

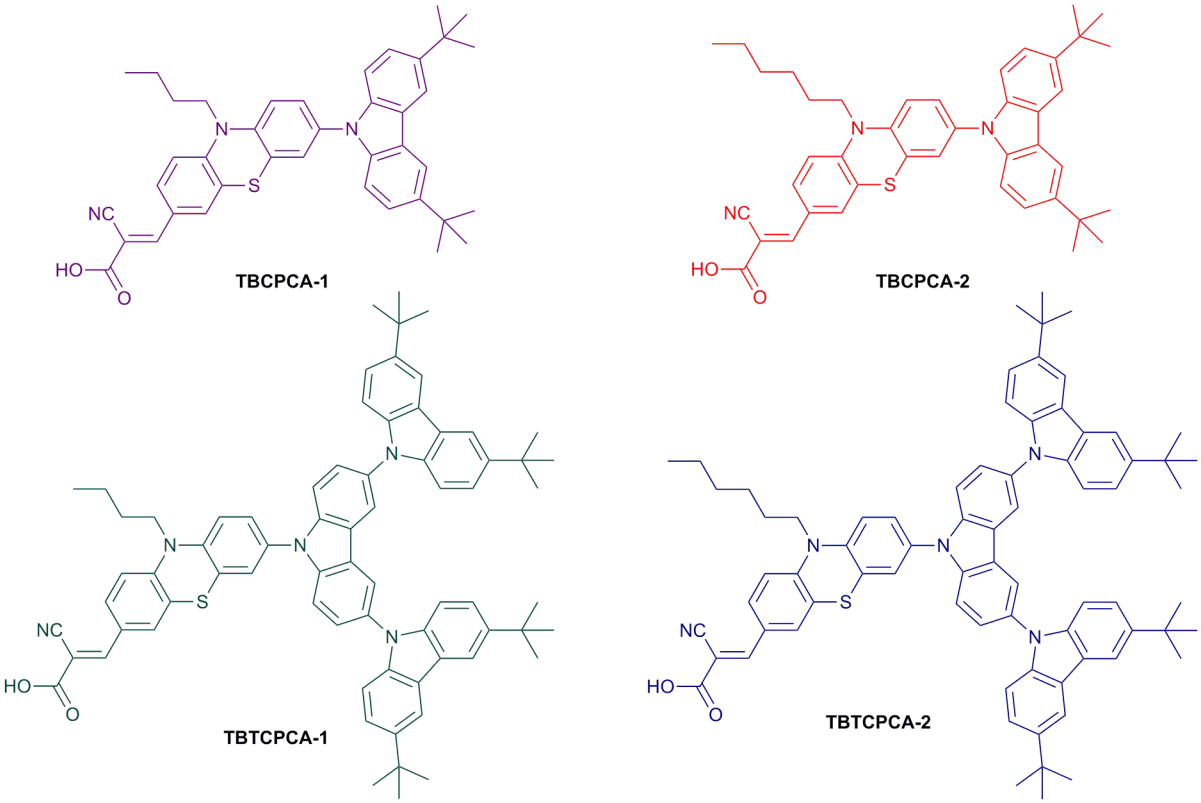

Figure 2. Structure of new metal free organic dyes **TBCPCA-1**, **TBCPCA-2**, **TBTCPCA-1** and **TBTCPCA-2**

ACCEPTED MANUSCRIPT

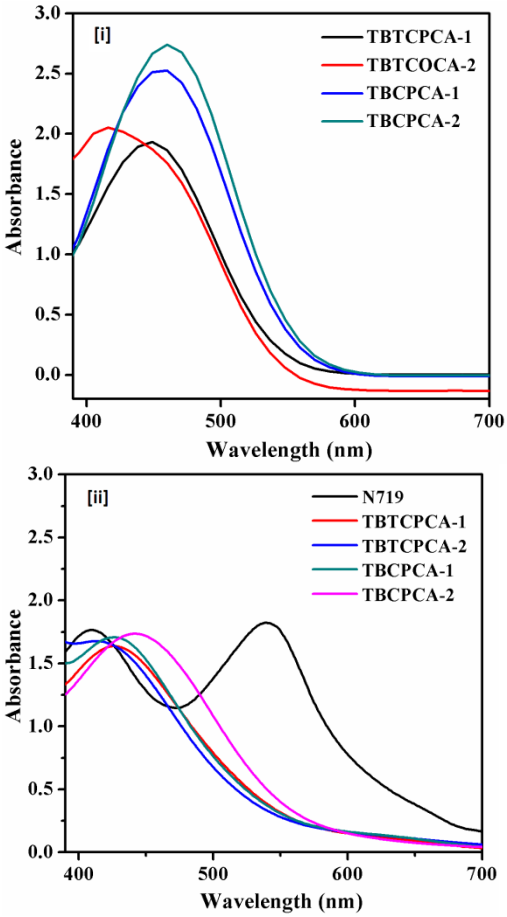

Figure 3. Absorption spectra of the metal free organic dyes **TBCPCA-1, TBCPCA-2, TBTCPCA-1** and **TBTCPCA-2** (i) in dichloromethane and (ii) on a nanocrystalline titania semiconductor.

ACCEPTED MANUSCRIPT

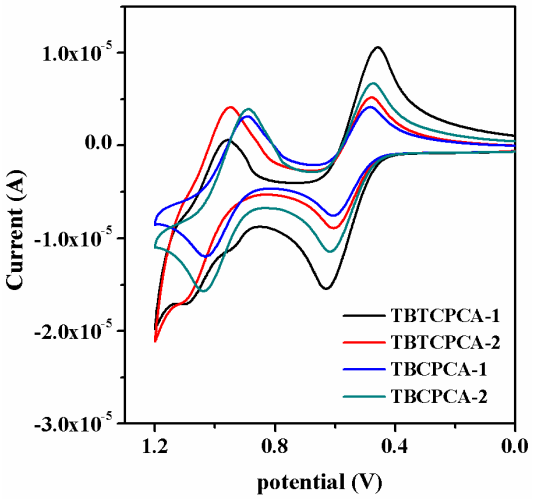

Figure 4. Cyclic voltamograms of the metal free dyes **TBCPCA-1**, **TBCPCA-2**, **TBTCPCA-1** and **TBTCPCA-2.**

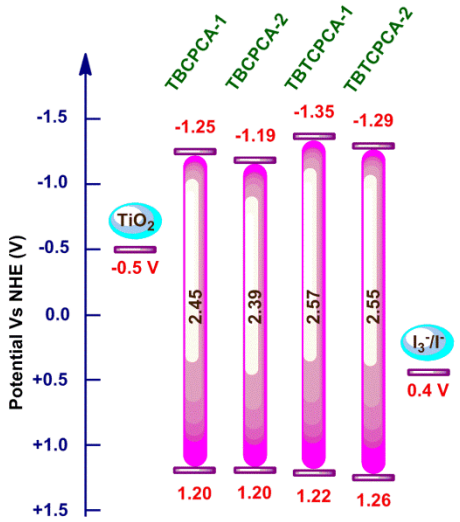

Figure 5. Energy level chart exhibiting the excited and ground state oxidation potentials resulted for the metal free dyes **TBCPCA-1**, **TBCPCA-2**, **TBTCPCA-1** and **TBTCPCA-2**.

ACCEPTED MANUSCRIPT

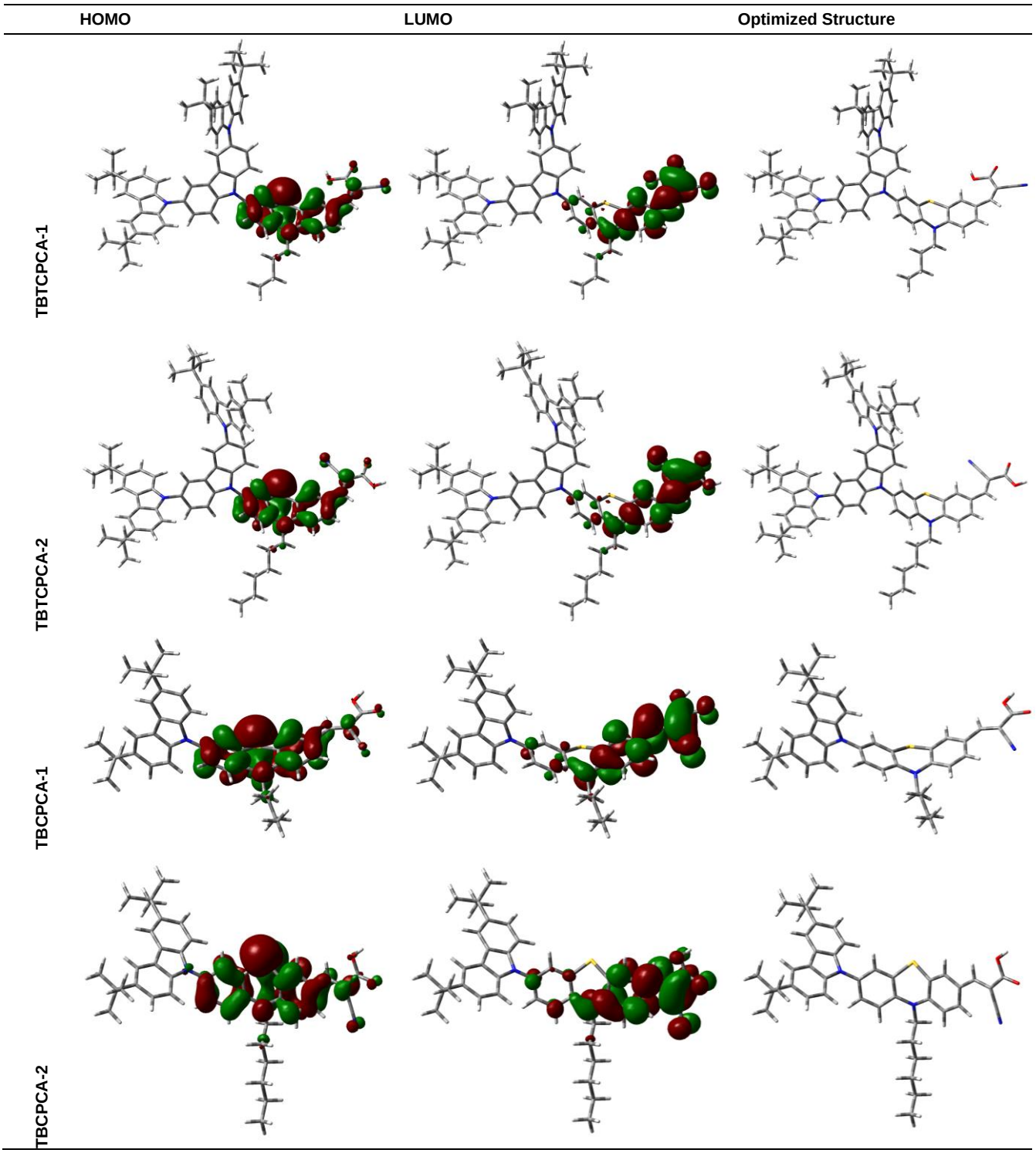

Figure 6. Electron distribution in the LUMOs and HOMOs for the metal free dyes **TBCPCA-1, TBCPCA-2, TBTCPCA-1** and **TBTCPCA-2.**

ACCEPTED MANUSCRIPT

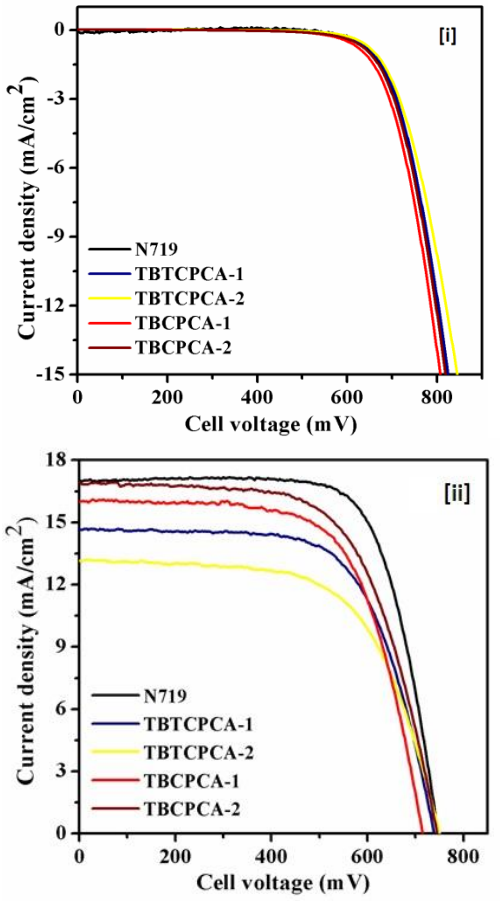

Figure 7. *J-V* Uniqueness of the fabricated DSSCs utilizing the metal free organic dyes **TBCPCA-1, TBCPCA-2, TBTCPCA-1** and **TBTCPCA-2** under (i) dark and (ii) at 100 mW cm-2 (AM 1.5G).

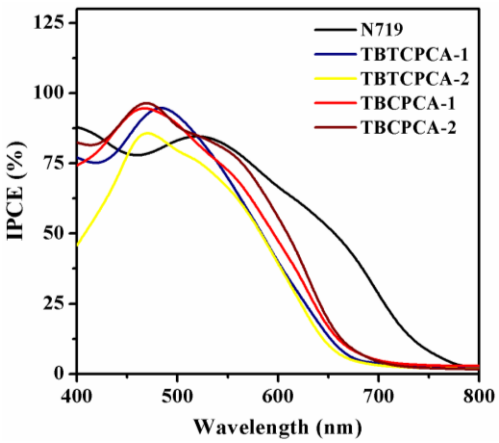

Figure 8. IPCE plots of the DSSCs fabricated utilizing the metal free organic dyes **TBCPCA-1, TBCPCA-2, TBTCPCA-1** and **TBTCPCA-2.**

ACCEPTED MANUSCRIPT

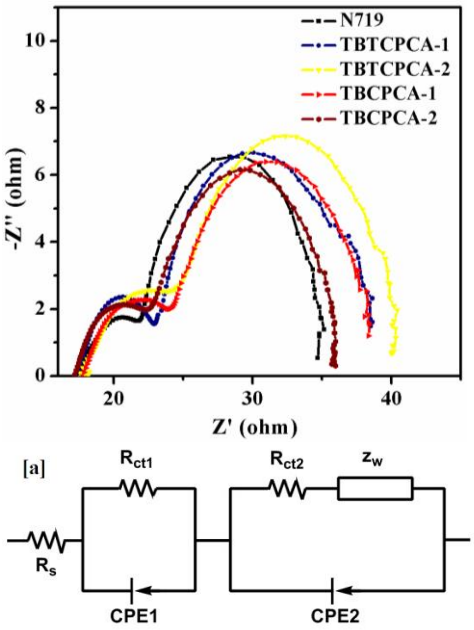

Figure 9. Nyquist plots resulted for the DSSCs under illumination conditions; (a) equivalent circuit.

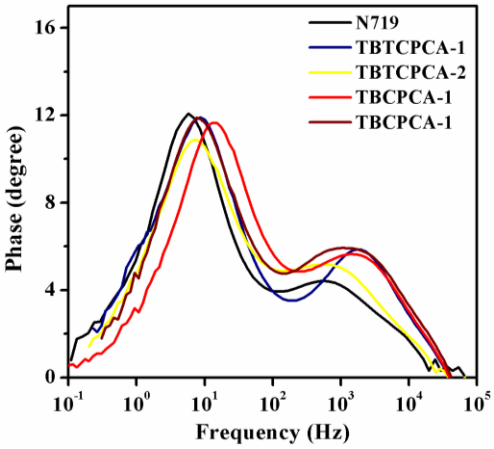

Figure 10. Bode phase plots for the DSSCs resulted under illumination conditions

ACCEPTED MANUSCRIPT

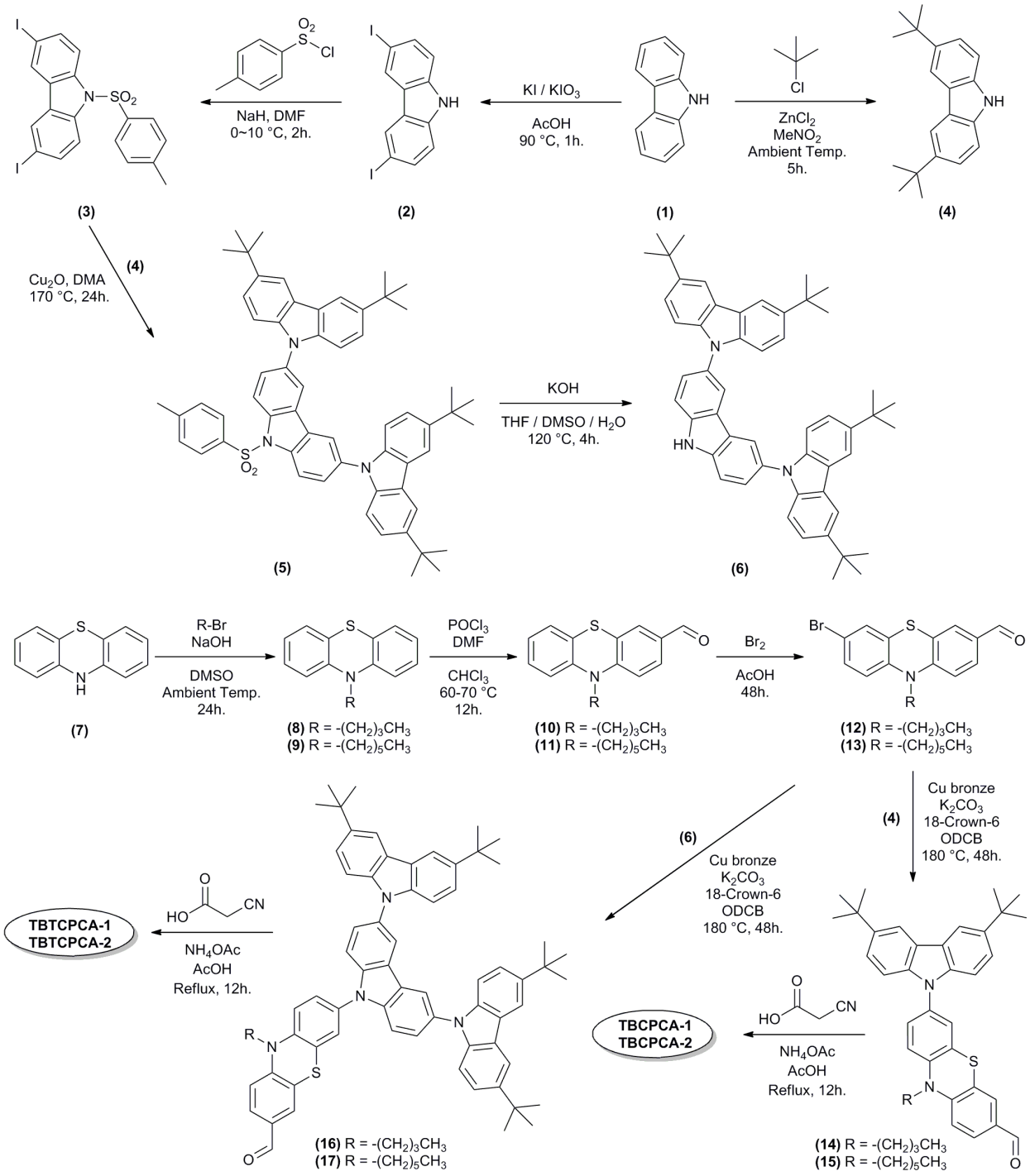

Scheme 1. Synthesis of new metal free organic dyes **TBCPCA-1**, **TBCPCA-2**, **TBTCPCA-1** and **TBTCPCA-2**

ACCEPTED MANUSCRIPT

Table 1. Optical/electrochemical statistics of the novel metal-free dyes **TBCPCA-1**, **TBCPCA-2**, **TBTCPCA-1** and **TBTCPCA-2.**

Dye	$\lambda_{max,}$nm (ε/ $M^{-1}cm^{-1}10^3$)	FWHM, nm	λ_{max} on TiO_2 nm	[a] E_{ox} (V)(ΔEp)	[b] HOMO (eV)	[c] LUMO (eV)	[d] E_{0-0} (eV)	[e] E_{0-0}^* (V)
TBCPCA-1	456 (12.66)	117.5	426	0.4244	5.2244	2.7789	2.4455	-1.251
TBCPCA-2	461 (13.70)	114.7	441	0.4244	5.2244	2.8355	2.3889	-1.954
TBTCPCA-1	448 (19.33)	124.3	426	0.4543	5.2543	2.682	2.5723	-1.348
TBTCPCA-2	417 (20.52)	167.5	413	0.4906	5.2906	2.7395	2.5511	-1.29

Absorption spectra were measured in DCM solution. [a] With reference to the ferrocene internal standard, redox potentials are reported. [b] Realized from the oxidation potential employing the formula HOMO = 4.8 + E_{ox}. [c] Acquired from the electrochemically deduced HOMO value and the optical band gap. [d] Calculated from the optical edge. [e] Oxidation potential (excited state) *versus* NHE.

Table 2. Photovoltaic performance parameters of the novel metal-free organic dyes incorporated DSSCs.

Dye	η (%)	V_{OC} (mV)	J_{SC} (mA/cm^2)	*ff*	f_{max} (Hz)	Electron lifetime, τ_e (ms)	R_{Ct2} (ohm)
TBCPCA-1	7.55±0.4	713±0.5	15.99±0.4	0.66±0.002	11.51	13.83	15.01
TBCPCA-2	7.97±0.3	745±0.6	16.92±0.3	0.67±0.003	5.72	27.82	14.21
TBTCPCA-1	7.11±0.3	739±0.5	14.68±0.2	0.68±0.002	7.56	21.05	15.71
TBTCPCA-2	6.17±0.4	745±0.6	13.11±0.3	0.66±0.002	5.72	27.82	16.21
N719	9.02±0.3	745±0.4	17.01±0.2	0.71±0.002	5.75	27.68	13.98